Available online at www.sciencedirect.com
SCIENCE DIRECT®
Journal of Organometallic Chemistry 690 (2005) 1265–1272
Journal of Organometallic Chemistry
www.elsevier.com/locate/jorganchem

Donor/acceptor organotriiron(II) hydrazone chromophores: structural, spectroscopic and electrochemical properties

Carolina Manzur [a,*], Lorena Millán [a], Mauricio Fuentealba [a], Jose A. Mata [b], David Carrillo [a,*], Jean-René Hamon [c,*]

[a] Laboratorio de Química Inorgánica, Instituto de Química, Pontificia Universidad Católica de Valparaíso, Avenida Brasil 2950, Valparaíso, Chile
[b] Departamento de Química Inorgánica y Orgánica, Universitat Jaume I, E-12080 Castellón, Spain
[c] UMR 6509 CNRS-Université de Rennes 1, Institut de Chimie de Rennes, Campus de Beaulieu, Bât. 10C, F-35042 Rennes-Cedex, France

Received 22 October 2004; accepted 18 November 2004
Available online 29 December 2004

Abstract

Two new trinuclear organoiron(II) complexes, in which a *trans*-1,2-ferrocenyl-ferrocenylene ethene unit (electron-donors) is attached to an electron-deficient cationic mixed sandwich via a conjugated hydrazone bridge, giving complexes of the type (*E*)-[CpFe(η^5-C_5H_4)–CH=CH–(η^5-C_5H_4)Fe(η^5-C_5H_4)–CH=NNH–(η^6-*p*-RC_6H_4)FeCp]$^+PF_6^-$ (Cp = η^5-C_5H_5; R = Me, **4**$^+PF_6^-$; MeO, **5**$^+PF_6^-$), have been prepared. The complexes were fully characterised by ^{1}H NMR, IR, UV–Vis spectroscopy. Their electrochemical properties have been studied by means of cyclic voltammetry, showing an effective electronic coupling between the two ferrocenyl fragments. The X-ray crystal structure of compound **4**$^+PF_6^-$ shows that it adopts the sterically more hindered *syn*-conformation about the 1,1′-ferrocenediyl core, with a parallel disposition of the conjugated dinucleating ligands, therefore, favouring an efficient electron delocalization through the entire π-framework. At the same time, the (C_5-ring)Fe moieties adopt an *anti*,*anti*-conformation with the iron atoms on the opposite faces of their respective bridging ligand.

Keywords: Sandwich complex; Cyclopentadienyl–iron complex; Arenehydrazone–iron complex; Electrochemistry; X-ray structure; Push–pull complex

1. Introduction

Since the discovery of ferrocene [1], a great deal of research effort has been expended on the study of bis (η^5-cyclopentadienyl)-metal complexes, and one of the richest areas of metallocene study has been that of linked ferrocenyl-type fragments [2,3]. Much of the interest in these species is concerned with the interaction between metal centres, since intermetallic electronic communication affords a wide range of new applications [3]. This has led to a large amount of studies devoted to describe the synthesis and electronic properties of new polymetallocenyl compounds [3,4], and regarding intramolecular electron-exchange reactions [5,6]. As part of our continuing study of interactions between remote electronically communicated metal centres, we recently reported synthesis and properties of new dinuclear organoiron(II) hydrazone complexes [7]. Such complexes combine the potent ferrocenyl electron-donating fragment with its electron-acceptor counterparts, the cationic mixed sandwich [CpFe(η^6-arene)]$^+$ moieties (Cp = η^5-C_5H_5), affording interesting bimetallic derivatives in

* Corresponding authors. Tel.: +33 (0) 223 235958; fax: +33 (0) 223 235637 (J.-R. Hamon), Fax: 56 32 27 34 20 (D. Carrillo, C. Manzur).
E-mail addresses: cmanzur@ucv.cl (C. Manzur), david.carrillo@ucv.cl (D. Carrillo), jean-rene.hamon@univ-rennes1.fr (J.-R. Hamon).

0022-328X/$ - see front matter © 2004 Elsevier B.V. All rights reserved.
doi:10.1016/j.jorganchem.2004.11.033

which the organometallic termini are connected by a conjugated hydrazone spacer (–NH–N=CH–).

In this article, we focuse our interest in the preparation, spectroscopic and structural characterisation, and electrochemical behaviour of two new trimetallic complexes in which one linked bisferrocenyl conjugated fragment, (*E*)-CpFe(η^5-C_5H_4)–CH=CH–(η^5-C_5H_4)Fe-(η^5-C_5H_4) = Fc–Fc, is attached to a [CpFe(η^6-*p*-R-arylhydrazone)]$^+$ moiety. These new triiron(II) derivatives have rich spectroscopic and electrochemical properties, containing two types of chromophore showing charge transfer behaviour which may be beneficial for the construction of nonlinear optical (NLO) materials [8], and three redox-active centre whose redox potentials will allow assessment of long-range metal–metal interactions across the conjugated bridges.

2. Results and discussion

2.1. Synthesis and characterisation

The new trinuclear hydrazone chromophores (*E*)-[Fc–Fc–CH=N–NH–(η^6-*p*-RC_6H_4)FeCp]$^+PF_6^-$ (R = Me, **4**$^+PF_6^-$; MeO, **5**$^+PF_6^-$) were successfully prepared by a condensation reaction of the ionic organometallic hydrazine precursors [CpFe(η^6-*p*-$RC_6H_4NHNH_2$)]$^+PF_6^-$ (R = Me, **1**$^+PF_6^-$; MeO, **2**$^+PF_6^-$) with the bis-ferrocene-based aldehyde building block (*E*)-Fc–Fc–CHO (**3**) [9], in refluxing ethanol solution containing catalytic amounts of concentrated acetic acid (Scheme 1). The two complexes were isolated as spectroscopically pure, air and thermally stable orange microcrystalline solids, in reasonable yields of 38% and 35%, respectively, after recrystallization from CH_2Cl_2 diethylether mixture. They exhibit a good solubility in common polar organic solvents, but are insoluble in diethylether, hydrocarbons and water. The identity of compounds **4**$^+PF_6^-$ and **5**$^+PF_6^-$ was authenticated by ^{1}H NMR, IR and UV–Vis spectroscopy (see Section 4.2. for the details), and additionally, by single crystal X-ray diffraction analysis of complex **4**$^+PF_6^-$ (vide infra).

The most remarkable common features observed in the solid state IR spectra of compounds **4**$^+PF_6^-$ and **5**$^+PF_6^-$ were: (i) a sharp medium absorption band at 3324 and 3333 cm^{-1}, respectively, attributed to the ν(NH) stretching vibration, (ii) a very weak band at 1610 cm^{-1} assigned to the ν(C=C) stretching mode, (iii) a strong band at 1570 and 1574 cm^{-1}, respectively, attributed to the stretching mode of the C=N group, (iv) a very strong $\nu(PF_6^-)$ band at 839 cm^{-1} for **4**$^+PF_6^-$, a splitting of this very strong band at 840 and 826 cm^{-1} for **5**$^+PF_6^-$, and (v) a strong δ(P–F) band at 557 and 558 cm^{-1}, respectively. Those stretching frequencies corroborate our previous observations with related organometallic hydrazones [7].

Interestingly, the unique set of signals observed in the ^{1}H NMR spectra (acetone-d_6, see Section 4.2.) clearly indicate the stereoselective formation of trinuclear organometallic hydrazones **4**$^+PF_6^-$ and **5**$^+PF_6^-$. The sterically less hindered *trans*-isomer about the N=C double bond is proposed in agreement with previous detailed NMR studies of their related bimetallic counterparts [CpFe(η^6-*p*-RC_6H_4)NHN=CH–(η^5-C_5H_4)FeCp]$^+PF_6^-$ (R = Me, **6**$^+PF_6^-$; MeO, **7**$^+PF_6^-$) [7d], and definitively assigned from the crystal structure of **4**$^+PF_6^-$ (see Section 2.2). The bis-ferrocene ethylene bridge signals of **5**$^+PF_6^-$ appear as an AB doublet at δ 6.39 and 6.51, whereas for **4**$^+PF_6^-$, only the doublet at δ 6.42 ppm is seen, the second doublet overlaps with the signal of the C_6H_4 ring protons. The characteristic $^3J_{H-H}$ coupling constant of 16 Hz is in accordance with a *trans* stereochemistry around the bridging C=C double bond. Both C_5H_5 resonances appear as singlets at δ 5.01–5.04 and 4.22–4.11 for the cationic and the neutral sandwiches, respectively. The proton resonances of the three magnetically inequivalent monosubstituted C_5H_4 rings appear for **4**$^+PF_6^-$, as four singlets integrating each for 3 H at δ 4.34–4.70, and for **5**$^+PF_6^-$ as six singlets integrating each for 2 H in the 4.20–4.69 ppm range. These signals appear to low field of the ferrocenyl C_5H_5 singlet,

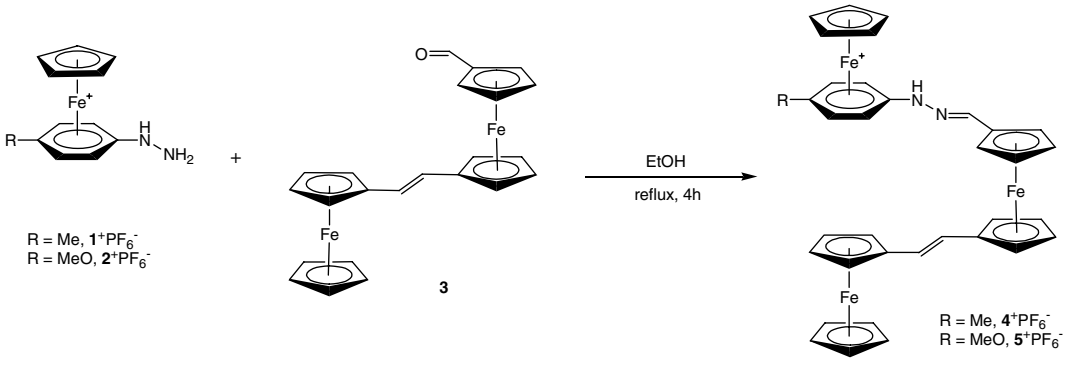

Scheme 1.

showing that all four ring protons are deshielded by the ethenediyl bridge and the imine functionality. The fact that we do not observe the characteristic A_2B_2 multiplets could result from the probable occurrence of several conformers in solution due to almost free rotation around the central ferrocenylene unit, i.e., of the two Cp rings one with respect to each other according to a "hinge-like" mechanism. The easiest conformer to pack is trapped during the crystallization process (see Section 2.2.). The upfield shifted aromatic protons of the coordinated C_6-ring (δ 6.14–6.22) and the deshielded methyne proton of the imine group (δ 7.93 and 7.91) appear in their respective expected regions [7d]. The low field position (δ 9.37 and 9.28) of the acidic benzylic NH [10] signal may be attributed to the electronic effect of the cationic organometallic moiety [11], and/or its participation in hydrogen-bonding with a fluoride of the PF_6^- counteranion (see Fig. 2).

The UV–Vis spectra of compounds $\mathbf{4}^+PF_6^-$ and $\mathbf{5}^+PF_6^-$, recorded in CH_2Cl_2, are very similar to those of their bimetallic counterparts $\mathbf{6}^+PF_6^-$ and $\mathbf{7}^+PF_6^-$ [7d]. They are consistent with most ferrocenylchromophores in that they exhibit two charge-transfer bands in the visible region [4,12]. The prominent band at 308 (sh 343) and 312 (sh 365) nm, respectively, is assigned to a ligand-centred π–π* electronic transition, and the less energetic and weaker band at 458 and 454 nm, respectively, responsible for the bright orange colour of the compounds, is attributed to a metal-to-ligand charge-transfer (MLCT) process (see Section 4.2). This assignment is in accordance with the latest theoretical treatment (model III) reported by Barlow *et al.* [13]. The bands associated with the d–d transitions of the cationic mixed sandwich [15] and of the ferrocenyl [16] entities are likely to be weaker and therefore buried under the two intense charge-transfer processes. No significant solvatochromic effect is observed when the spectra are recorded in DMSO (see Section 4.2. for details).

2.2. X-ray crystallographic studies

The single crystal X-ray diffraction study of the trimetallic hydrazone complex (*E*)-[CpFe(η^5-C_5H_4)–CH=CH–(η^5-C_5H_4)Fe(η^5-C_5H_4) – CH=NNH–(η^6-*p*-MeC_6H_4)FeCp]$^+PF_6^-$ ($\mathbf{4}^+PF_6^-$), was undertaken and the crystal structure was determined as outlined in Section 4.3. The ORTEP plot of the cationic organometallic entity $\mathbf{4}^+$ with the atom labeling scheme is presented in Fig. 1, and selected intramolecular distances and angles are listed in Table 1. Compound $\mathbf{4}^+PF_6^-$ crystallizes in the orthorhombic space group *Pbca* with eight molecules in the unit cell. In the mixed sandwich fragment, the iron atom is coordinated to the cyclopentadienyl ring at a ring centroid-iron distance of 1.662 Å, and to the aryl ring at a ring centroid-iron distance of 1.544 Å. In the central ferrocenylene subunit, the iron atom is coordinated to the cyclopentadienyl rings at a ring centroid-iron distances of 1.648 and 1.651 Å, and in the terminal ferrocenyl moiety the iron atom is coordinated to the cyclopentadienyl rings at a ring centroid-iron distances of 1.654 and 1.643 Å for the substituted and the unsubstituted ring, respectively. These metrical parameters

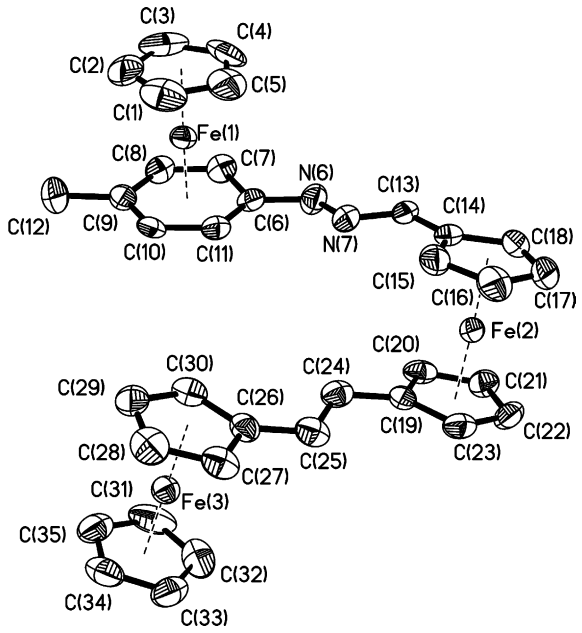

Fig. 1. Molecular structure and atom numbering scheme for $\mathbf{4}^+PF_6^- \cdot CH_2Cl_2$. Hydrogen atoms, the PF_6^- counteranion, and the solvent molecule have been omitted for clarity. Displacement ellipsoids are at the 35% probability level.

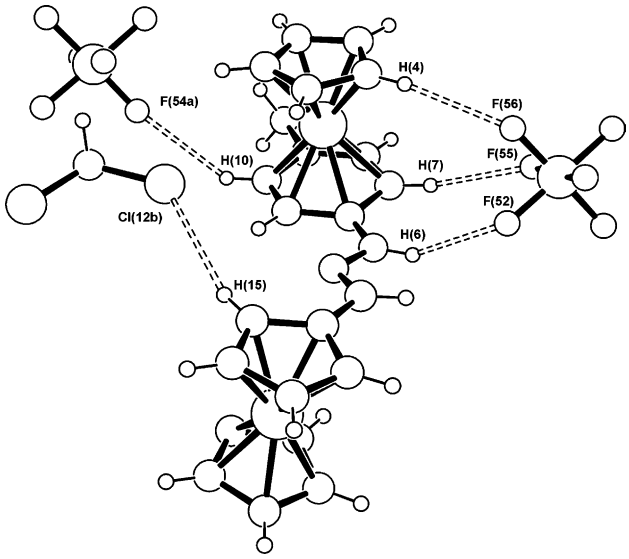

Fig. 2. Ball and stick view of hydrogen-bonding interactions between the cationic organometallic framework $\mathbf{4}^+$ and the PF_6^- counteranion and the CH_2Cl_2 solvate. For clarity, only the interacting atoms have been labelled, and the CpFe(η^5-C_5H_4)–CH=CH– fragment of $\mathbf{4}^+$ has been omitted.

Table 1
Bond distances (Å) and angles (°) for $4^{+}PF_6^{-} \cdot CH_2Cl_2$[a]

Bond distances			
Fe(1)–C(6)	2. 141(8)	C(6)–N(6)	1. 380(10)
Fe(1)–C(7–11)[b]	2.073	N(6)–N(7)	1. 371(9)
C(13)–C(14)	1.446(11)	N(7)–C(13)	1. 279(9)
Fe(2)–C(14–18)[b]	2.040	Fe(2)–C(19–23)[b]	2.039
Fe(3)–C(26–30)[b]			
Fe(1)–C(1–5)[b]			
C(19)–C(24)			
Bond angles			
C(6)-N(6)–N(7)	119.9(7)	N(6)–N(7)–C(13)	115.8(7)
N(7)–C(13)–C(14)	121.5(8)	C(19)–C(24)–C(25)	125.5(8)
C(24)–C(25)–C(26)	126.4(8)	Cp_{CNT}–Fe(1)–Ph_{CNT}	178.17
Cp'_{CNT}–Fe(2)–Cp'_{CNT}	178.38	Cp_{CNT}–Fe(3)–Cp'_{CNT}	178.35

[a] Abbreviations: Cp, η^5-C_5H_5; Cp′, η^5-C_5H_4; Ph, η^6-C_6H_4; CNT, centroid.
[b] Average distance.

together with those listed in Table 1 are similar to those we have already reported for bimetallic hydrazone complexes [7a,7c–7e], and are typical of η^5-Fe-η^6 and η^5-Fe-η^5 metallocene-type coordination [16]. The complexes show a perfect eclipsed disposition of the Cp rings in the two ferrocene units, and a weak tilting angle is observed between the two Cp rings of each ferrocenyl unit. The ring centroid-iron-ring centroid angles are indeed of 178.38° and 178.35° for the central ferrocenylene and the terminal ferrocenyl subunits, respectively. This angle is of 178.17° for the mixed sandwich $[CpFe(\eta^6\text{-}p\text{-}MeC_6H_4)]^+$.

As shown in Fig. 1, the cationic organometallic moiety $\mathbf{4}^+$ adopts an *anti*-conformation with the two iron Fe(1) and Fe(2) atoms on the opposite faces of the dinucleating planar hydrazonyl ligand $[p\text{-}MeC_6H_4\text{–}NHN{=}CH\text{–}C_5H_4]^-$. The dihedral angle between C_6- and C_5-ring planes is 12.94°. The through-bond and through-space Fe···Fe distances are of 9.662 and 7.491 Å, respectively. As already seen in the crystal structures of the starting bis-ferrocene-based aldehyde **3** and of its trimetallic derivatives (*E*,*E*)-Fc–Fc–CH=CH–C_5H_4N–$M(CO)_5$ (M = Cr, Mo, W) [9], the bis-ferrocene fragment in $\mathbf{4}^+$ adopts also the *anti*-conformation with a dihedral angle of 8.50° between the two C_5-ring planes of the dinucleating (*E*)-$[C_5H_4\text{–}CH{=}CH\text{–}C_5H_4]^{2-}$ ligand. The through-bond and through-space Fe(2)···Fe(3) distances are 8.347 and 7.195 Å, respectively. As for the 1,1′-bis-substituted ferrocenyl complexes reported so far in the literature [9,17], $\mathbf{4}^+$ adopts the sterically more hindered conformation with a parallel disposition of the ancillary ligands (see Fig. 1), in which intramolecular π-stacking could have some effect. However, in the cases of $\mathbf{4}^+$, of the organometallic aldehyde (*E*)-Fc–Fc–CHO **3** [9], and of the bimetallic ferrocenyl 1,1′-bis-substituted hydrazone complex (*E*)-$[CpFe(\eta^6\text{-}p\text{-}MeC_6H_4)NHN{=}CH(\eta^5\text{-}C_5H_4)Fe(\eta^5\text{-}C_5H_4)\text{–}CH{=}CH\text{–}C_6H_4\text{-}p\text{-}Me]^+PF_6^-$ [7a], where π-stacking is not possible, the same hindered conformation is also observed. This indicates that packing effects may be having a more important influence in the steric disposition of the molecule in the crystal. Moreover, the dihedral angle of 53.90° between the C(6-11), C(14-18), C(19-23) and C(26-30) ring centroids nicely Illustrates a "hinge-like" behaviour of the central ferrocenylene unit.

On the other hand, a careful examination of Table 1 reveals some interesting structural features provoked by the strong electron withdrawal $CpFe^+$ moiety on the arene ligand. Thus, the Fe(1)–C(6) bond length, 2.141(8) Å, is longer than the mean value of the other five Fe(1)–C(C_6-ring) bond lengths (2.073 Å). Such a Fe–C elongation is a characteristic feature of the hexahapto coordinated arylhydrazones [7a,7c–7e,10b,18]. This elongation is a consequence of a partial delocalization of the N(6) electron lone-pair toward the mixed sandwich moiety and is reflected by (i) a depyramidalization of the N(6) atom with typical bond angles at this sp^2-hybridized nitrogen atom (C(6)–N(6)–N(7) = 119.9(7)°), (ii) a C(6)–N(6) bond length of 1.380(10) Å which is intermediate between a single and a double carbon nitrogen bond [16], and (iii) a slight cyclohexadienyl-like character of the coordinated phenyl ring with a folding dihedral angle of 4.57(3)° about the C(7)–C(11) axis.

Finally, the structure of the cationic moiety $\mathbf{4}^+$ is completed by a PF_6^- counter-anion and a molecule of CH_2Cl_2 that are both involved in hydrogen-bonding interactions (see Fig. 2). As expected from our previous observations [7c], the acidic benzylic hydrogen H(6) interacts strongly with fluorine F(52) with a F(52)···N(6) length/angle of 2.962(11) Å/147°, and a F(52)···H(6) separation of 2.20 Å. The PF_6^- anion is also weakly coupled to the organometallic cation $\mathbf{4}^+$ through the H(4)···F(56), H(7)···F(55), and H(10)···F(54a) hydrogen-bonding interactions (Table 2). The crystallization solvent is also implied in the stabilization of the structure through a close contact of 2.82 Å

Table 2
Hydrogen-bonding interaction parameters for $\mathbf{4}^{+}PF_6^{-} \cdot CH_2Cl_2$

D–$H\cdots A$	$D\cdots A$ (Å)	$H\cdots A$ (Å)	D–$H\cdots A$ (°)
N(6)–H(6)···F(52)	2.962(11)	2.20	147
C(4)–H(4)···F(56)	3.386(16)	2.49	162
C(7)–H(7)···F(55)	3.305(15)	2.40	165
C(10)–H(10)···F(54a)[a]	3.321(14)	2.54	142
C(15)–H(15)···Cl(2b)[a]	3.706(10)	2.82	159

[a] Symmetry transformations used to generate equivalent atoms: (a) $1 + x, y, z$; (b) $3/2 - x, -1/2 + y, z$.

measured between H(15) and one chlorine atom (Cl(2b)) of the dichloromethane molecule.

2.3. Electrochemical studies

In order to get a deeper insight into the mutual donor–acceptor electronic influence with respect to electrochemical perturbations, we have undertaken the cyclic voltammetry (CV) study of the homotrimetallic hydrazone complexes $\mathbf{4}^{+}PF_6^{-}$ and $\mathbf{5}^{+}PF_6^{-}$. All the cyclovoltammograms were recorded in acetonitrile using the same setup (see Section 4.1.), and the resulting electrochemical data are summarized in Table 3. The trinuclear complexes $\mathbf{4}^{+}PF_6^{-}$ and $\mathbf{5}^{+}PF_6^{-}$ contain two ferrocene and one [CpFe^{+}(arene)]-type fragment, the three of which are redox active. They display two major features: (i) an irreversible process attributable to Fe-centered reduction at the mixed sandwich fragment [14a,19], and (ii) two chemically reversible ferrocene-based redox couples (the cathodic and anodic peak currents are equal and the waves are symmetric) [20], corresponding to the oxidation of the terminal ferrocenyl and of the bridging ferrocenylene subunits (Fig. 3). The peak to peak separations (ΔE_p) are, however, significantly greater than the ideal value of 60 mV for a fully reversible one-electron process. This may be ascribed to a combination of uncompensated solution resistance and slightly slow

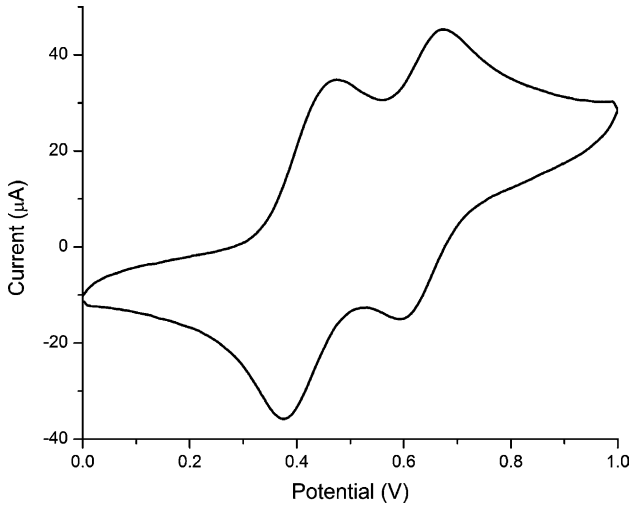

Fig. 3. Cyclic voltammograms (oxidation side) of Complex $\mathbf{4}^{+}PF_6^{-}$, recorded in acetonitrile/0.1 M $n-Bu_4N^{+}PF_6^{-}$ at $T = 293$ K and a voltage sweep rate $v = 0.1$ V s^{-1}, reference electrode Ag/AgCl, internal reference $Cp_2Fe^{0/+}$.

electron-transfer kinetics [21]. Unsubstituted ferrocene under the same conditions gave ΔE_p values of 84 mV.

As can be seen in Table 3, the redox waves corresponding to the two ferrocenyl fragments of $\mathbf{4}^{+}PF_6^{-}$ and $\mathbf{5}^{+}PF_6^{-}$ are strongly influenced by the electron withdrawing nature of the ancillary cationic mixed sandwich. The first oxidation in each case corresponds to oxidation of the more electron releasing terminal ferrocenyl unit, and the second wave corresponds to the oxidation of the central ferrocenylene unit. These assignments were made by analogy to the oxidation potentials of their respective bimetallic counterparts $\mathbf{6}^{+}PF_6^{-}$ and $\mathbf{7}^{+}PF_6^{-}$, and their relative position with respect to the ferrocene/ferrocenium couple. Like for the starting aldehyde material **3** [9], the half wave potential of the ferrocenyl moieties show a clear anodic shift (120–130 mV) compared to the parent complex Fc–CH=

Table 3
Electrochemical data[a]

Compound	$E_{1/2}$[b] (V) (ΔE_p[c] (mV)) ferrocene-based	ΔE[d] (mV)	K_c[e]	E_p[f] CpFe^{+}(arene)-based	Ref.
3	0. 405 (90), 0. 785 (85)	380	2.6×10^6	–	[9]
$\mathbf{4}^{+}PF_6^{-}$	0.418 (96), 0.631 (90)	213	4075	−2.06	This work
$\mathbf{5}^{+}PF_6^{-}$	0.406 (83), 0.633 (86)	227	7038	−1.88	This work
$\mathbf{6}^{+}PF_6^{-}$	0.570 (89)	–	–	−1.46	[7d]
$\mathbf{7}^{+}PF_6^{-}$	0.560 (68)	–	–	−1.38	[7d]
Fc–CH=CH–	290	170	700	–	[22]
Fc	460				
Cp_2Fe	0.440 (84)	–	–	–	This work

[a] Recorded in MeCN at 298 K with 0.1 M n-$Bu_4N^{+}PF_6^{-}$ as supporting electrolyte; all potentials are vs. Ag/AgCl; scan rate = 0.1 V s^{-1}.
[b] Potentials are taken as the midpoints between anodic and cathodic peaks.
[c] Peak-to-peak separation between the resolved reduction and oxidation wave maxima.
[d] $\Delta E = E_{1/2}(Fc^{+}\text{–}Fc^{+}) - E_{1/2}(Fc\text{–}Fc^{+})$.
[e] ΔE (mV) = 59.15 ($\log K_c$) at 298 K.
[f] Peak potential of the irreversible wave corresponding to the reduction of the [CpFe(arene)]$^{+}$ fragment.

CH–Fc [22], indicating some degree of electronic interaction between the iron centres and the electron-accepting fragment. The presence of two one-electron oxidations, instead of one two-electron oxidation, indicates a stabilization of the mixed-valence species. From this wave splitting ΔE (Eq. (1)), the comproportionation constants K_c relative to the equilibrium of Eq. (2) can be computed (Eq. (3)), and are reported in Table 3

$$\Delta E = E_{1/2}(Fc^{+}\text{–}Fc^{+}) - E_{1/2}(Fc\text{–}Fc^{+}) \quad (1)$$

$$Fc\text{–}Fc + Fc^{+}\text{–}Fc^{+} \overset{K_c}{\rightarrow} 2Fc\text{–}Fc^{+} \quad (2)$$

$$\Delta E\ (\mathrm{mV}) = 59.15(\log K_c) \quad \text{at } 298\ \mathrm{K} \quad (3)$$

This remains, however, a crude estimation of the electronic interaction between the iron centres due to their geometrical intrinsic inequivalency. Such an approximation has also been used in some other examples in metal–metal carbon bridged asymmetric homobimetallic [9,23] and heterobimetallic complexes [24].

In addition, the two compounds studied undergo an irreversible reduction step centered at the mixed sandwich moiety, corresponding to the single-electron reduction of the d^6, Fe(II), 18-electron complexes to the unstable d^7, Fe(I), 19-electron species [14b,19]. Their very cathodic potentials (Table 3) are very similar to those reported for the monometallic benzaldehyde-hydrazone complexes [10b], and are presumably due to the reduction of an in situ generated neutral zwitterionic species [10]. Nevertheless, the electrochemical data make clear that in these trinuclear hydrazone complexes the nature of the HOMO is still dominated by the neutral donating bis-ferrocenyl units, whereas the character of the LUMO is determined by the cationic mixed sandwich, in accordance with previous experimental and theoretical work [7d].

3. Concluding remarks

We have prepared and fully characterised two trinuclear organoiron(II) complexes in which a *trans*-1,2-ferrocenyl-ferrocenylene ethene fragment (electron-donors) has been attached to an electron-deficient cationic mixed sandwich via a conjugated hydrazone bridge. The coplanar and parallel arrangement of the two dinucleating ligands acting at the ferrocenylene "hinge" might allow an efficient electron delocalization or electronic interaction between the electron-donating and electron-accepting termini through the entire π-conjugated framework. These complexes therefore have the basic architectural and electronic properties necessary to exhibit second-order non-linear optical (NLO) behaviour. Other complexes based on attachment of electron donors to $[CpFe(\eta^6\text{-aryl})]^+$ moiety via π-conjugated spacer have indeed been shown to have significantly high values of the molecular hyperpolarisability β [25]. Although complex $\mathbf{4}^{+}PF_6^{-}$ crystallises in a centrosymmetric space group and cannot therefore show second-order non-linear properties in the bulk solid state, the β values for the individual molecules may still be substantial. The NLO measurements will be the subject of a separate report.

4. Experimental

4.1. General remarks

The reactions were accomplished using standard Schlenk-line techniques under an atmosphere of dinitrogen. Solvents were dried and distilled under dinitrogen by standard methods prior to use. Solid IR spectra were obtained from KBr disks on a Perkin–Elmer, Model Spectrum One, FT IR spectrophotometer. Electronic spectra were recorded in CH_2Cl_2 and DMSO solutions on a Spectronic, Genesys 2, spectrophotometer. The ^1H NMR spectra were recorded on an Avance 400 Digital NMR Bruker spectrometer (400 MHz) at 297 K, and all chemical shifts are quoted in ppm, relative to internal tetramethylsilane (TMS). Cyclic voltammetry experiments were performed at room temperature with a Radiometer PGZ100 potentiostat, using a standard three-electrode setup with a vitreous carbon working and platinum wire auxiliary electrodes and a Ag/AgCl electrode as the reference electrode. Acetonitrile solutions were 1.0 mM in the compound under study and 0.1 M in the supporting electrolyte $n\text{-}Bu_4N^{+}PF_6^{-}$ with a voltage scan rate = 100 mV s^{-1}. The Cp_2Fe/Cp_2Fe^{+} couple was used as an internal reference for the potential measurements. Melting points were determined in evacuated capillaries and were not corrected. The organometallic hydrazine precursors $[CpFe(\eta^6\text{-}p\text{-}RC_6H_5\text{-}NHNH_2)]^{+}PF_6^{-}$, (R = Me, $\mathbf{1}^{+}PF_6^{-}$; MeO, $\mathbf{2}^{+}PF_6^{-}$) were synthesized as previously described [18c]. The 1,2-bis-ferrocenylethene carboxaldehyde (*E*)-$[CpFe(\eta^5\text{-}C_5H_4)\text{–}CH{=}CH\text{–}(\eta^5\text{-}C_5H_4)Fe(\eta^5\text{-}C_5H_4)\text{–}CHO]$, (**3**), was prepared according to published procedures [9]. All other reagents were purchased from commercial sources and used as received.

4.2. Preparation of hydrazone complexes

4.2.1. General procedure

The Schlenk tube was charged with a solid sample of the ionic organometallic hydrazine $[CpFe(\eta^6\text{-}p\text{-}RC_6H_4\text{-}NHNH_2)]^{+}PF_6^{-}$ (R = Me, $\mathbf{1}^{+}PF_6^{-}$; MeO, $\mathbf{2}^{+}PF_6^{-}$), an equivalent molar amount of the 1,2-bis-ferrocenylethene carboxaldehyde, (*E*)-$[CpFe(\eta^5\text{-}C_5H_4)\text{–}CH{=}CH\text{–}(\eta^5\text{-}C_5H_4)Fe(\eta^5\text{-}C_5H_4)\text{–}CHO\}$, (**3**), 5 ml of EtOH containing 2 drops of acetic acid as catalyst, and a magnetic stirring bar. The reaction mixture was stirred and

refluxed for 4 h under dinitrogen. After cooling to room temperature, the solution was layered with diethyl ether and then stored at −30 °C overnight. The precipitated solid was filtered on a fritted glass funnel, washed twice with 5 mL of diethyl ether and dried under vacuum before being recrystallized from a CH_2Cl_2/Et_2O mixture (1:1).

4.2.2. (E)-[CpFe(η^5-C_5H_4)–CH=CH–(η^5-C_5H_4)Fe-(η^5-C_5H_4)–CH=NNH–(η^6-p-MeC_6H_4)FeCp]$^+PF_6^-$, ($\mathbf{4}^+PF_6^-$)

$\mathbf{1}^+PF_6^-$: 56.0 mg (0.15 mmol), **3**: 63.0 mg (0.15 mmol). Yield: 38% (45 mg) of orange-red microcrystals. M.p.: 235 °C (dec). UV–Vis (λ_{max} (logε)): (CH_2Cl_2) 237 (4.45), 308 (4.36), 343 (3.71), 458 (3.63); (DMSO) 308 (4.31), 347 (3.84), 454 (3.57). IR (KBr, cm^{-1}): 3324w ν(NH); 3080w, 2957vw, 2920vw, 2848vw ν(CH); 1610vw ν(C=C); 1570m ν(C=N); 839vs ν(PF_6), 557m δ(PF). ^{1}H NMR (acetone-d_6): δ 2.49 (s, 3H, CH_3), 4.22 (broad s, 5H, CpFe), 4.34 (s, 3H, C_5H_4), 4.44 (s, 3H, C_5H_4), 4.51 (s, 3H, C_5H_4), 4.70 (s, 3H, C_5H_4), 5.01 (s, 5H, $CpFe^+$), 5.64 (s, 2H, CH_2Cl_2), 6.22 (broad s, 5H, C_6H_4 + CH=CH), 6.42 (d, 1H, $^3J_{HH}$ = 16.2 Hz, C*H*=C*H*), 7.93 (s, 1H, N=C*H*), 9.37 (s, 1H, N*H*).

4.2.3. (E)-[CpFe(η^5-C_5H_4)–CH=CH–(η^5-C_5H_4)-Fe(η^5-C_5H_4)–CH=NNH–(η^6-p-$MeOC_6H_4$)FeCp]$^+PF_6^-$, ($\mathbf{5}^+PF_6^-$)

$\mathbf{2}^+PF_6^-$: 29.0 mg (0.071 mmol), **3**: 30 mg (0.071 mmol). Yield: 35% (20 mg) of orange-brown microcrystals. M.p. 226 °C (dec). UV–Vis (λ_{max} (logε)): (CH_2Cl_2) 236 (4.47), 312 (4.41), 365 (3.04), 456 (3.62). (DMSO) 310 (4.35), 348 (3.67), 455 (3.62). IR (KBr, cm^{-1}): 3333w ν(NH); 3087vw, 2964vw, 2920vw, 2848vw ν(CH); 1610vw ν(C=C); 1574w ν(C=N); 1252m ν(CH_3O); 840vs, 826vs ν (PF_6), 558m δ(PF). ^{1}H NMR (acetone-d_6): δ 4.03 (s, 3H, CH_3O), 4.11 (broad s, 5H, CpFe), 4.20 (s, 2H, C_5H_4), 4.33 (s, 2H, C_5H_4), 4.38 (s, 2H, C_5H_4), 4.44 (s, 2H, C_5H_4), 4.53 (s, 2H, C_5H_4), 4.69 (s, 2H, C_5H_4), 5.04 (s, 5H, $CpFe^+$), 6.14 (d, 2H, $^3J_{HH}$ = 6.8 *Hz*, C_6H_4), 6.21 (d, 2H, $^3J_{HH}$ = 6.8 *Hz*), 6.39 (d, 1H, $^3J_{HH}$ = 16.1 *Hz*, C*H*=C*H*), 6.51 (d, 1H, $^3J_{HH}$ = 16.1 *Hz*, C*H*=C*H*), 7.91 (s, 1H, N=C*H*), 9.28 (s, 1H, N*H*).

4.3. X-ray crystallographic study of $\mathbf{4}^+PF_6^- \cdot CH_2Cl_2$

Suitable crystals for X-ray diffraction studies were grown by slow diffusion of diethyl ether into a concentrated CH_2Cl_2 solution of $\mathbf{4}^+PF_6^-$ at room temperature. An orange plate of this complex having dimensions of $1.52 \times 0.16 \times 0.05$ mm was mounted on a glass fiber in a random orientation. Data collection was performed at room temperature on a Siemens Smart CCD diffractometer using graphite monochromated Mo Kα radiation (λ = 071073 Å) with a nominal crystal-to-detector distance of 4.0 cm. A hemisphere of data was collected on the basis of three ω-scans runs (starting $\omega = -28°$) at values $\varphi = 0°$, 90°, 180°, with the detector at $2\theta = 28°$. In each of these runs, frames (606, 435, 230, respectively) were collected at 0.3° intervals and for 40 s per frame. The diffraction frames were integrated using the SAINT package and corrected for absorption with SADABS [26,27]. The positions of the heavy atoms were determined by direct method and successive difference electron density maps using the SHEXTL 5.10 software package [28] were done to locate the remaining atoms. Refinement was performed by the full-matrix least-squares method based on F^2. All non-hydrogen atoms were refined anisotropically. The positions of the aromatic hydrogens were generated geometrically, assigned isotropic thermal parameters and allowed to ride on their respective parent C atoms.

Crystallographic data for $\mathbf{4}^+PF_6^- \cdot CH_2Cl_2 : C_{36}H_{35}Cl_2F_6Fe_3N_2P$, Mr = 879.08 g mol^{-1}, unit cell dimensions: a = 10.8172(10), b = 14.9939(14), c = 44.288(4) Å, V = 7183.1(12) Å^3, orthorhombic, *Pbca*, Z = 8, D_{calcd} = 1.626 g cm^{-3}, μ = 1.450 mm^{-1}, SADABS absorption correction applied, $F(000)$ = 3568, T = 298 (2) K, 2θ max: 54°, reflections collected/unique/used: 29 010/4392/4392 ($I > 2\sigma(I)$), parameters refined: 451, R/R_{w2} ($I > 2\sigma(I)$) = 0.0600/0. 1457, R/R_{w2} (all data) = 0.0966/0.1718, GOF = 1.005, $[\Delta\rho]_{min}/[\Delta\rho]_{max}$: −0.448/0.652.

5. Supplementary material

Crystallographic data (excluding structure factors) for the structural analysis have been deposited with the Cambridge Crystallographic Data Centre as supplementary publication CCDC-243751. Copies of this information may be obtained free of charge from The Director, CCDC, 12 Union Road, Cambridge CB2 1EZ, UK (fax: +44-1223-336-033; e-mail: deposit@ccdc.cam.ac.uk or www: http://www.ccdc.cam. ac.uk).

Acknowledgements

The authors gratefully acknowledge Fondo Nacional de Desarrollo Científico y Tecnológico, FONDECYT (Chile), Grant No. 1010318 (D.C., C.M.), the Programme International de Coopération Scientifique, CNRS-CONICYT No. 16771 (C.M., D.C., J.-R.H.), the Pontificia Universidad Católica de Valparaíso, the Universitat Jaume I, and the Université de Rennes 1 for financial support.

References

[1] (a) T.J. Kealy, P.L. Pauson, Nature 168 (1951) 1039;
(b) S.A. Miller, J.A. Tebboth, J.F. Tremaine, J. Chem. Soc. (1952) 632;
(c) G. Wilkinson, J. Organomet. Chem. 100 (1975) 273.

[2] (a) D.O. Cowan, C. LeVanda, J. Park, F. Kaufman, Acc. Chem. Res. 6 (1973) 1;
(b) U.T. Muller-Westerhoff, Angew. Chem., Int. Ed. Engl. 25 (1986) 702.
[3] S. Barlow, D. O'Hare, Chem. Rev. 97 (1997) 637, and references therein.
[4] E. Peris, Coord. Chem. Rev. 248 (2004) 279, and references therein.
[5] D. Astruc, Electron Transfer and Radical Reactions in Transition-Metal Chemistry, VCH, New York, 1995.
[6] J.-P. Launay, Chem. Soc. Rev. 30 (2001) 386, and references therein.
[7] (a) C. Manzur, C. Zúñiga, L. Millán, M. Fuentealba, J.A. Mata, J.-R. Hamon, D. Carrillo, New J. Chem. 28 (2004) 134;
(b) A. Trujillo, M. Fuentealba, C. Manzur, D. Carrillo, J.-R. Hamon, J. Organomet. Chem. 681 (2003) 150;
(c) C. Manzur, M. Fuentealba, L. Millán, F. Gajardo, M.T. Garland, R. Baggio, J.A. Mata, J.-R. Hamon, D. Carrillo, J. Organomet. Chem. 660 (2002) 71;
(d) C. Manzur, M. Fuentealba, L. Millán, F. Gajardo, D. Carrillo, J.A. Mata, S. Sinbandhit, P. Hamon, J.-R. Hamon, S. Kahlal, J.-Y. Saillard, New J. Chem. 26 (2002) 213;
(e) C. Manzur, M. Fuentealba, D. Carrillo, D. Boys, J.-R. Hamon, Bol. Soc. Chil. Quim. 46 (2001) 409.
[8] See for example (a): C.E. Powell, M.G. Humphrey, Coord. Chem. Rev. 248 (2004) 725;
(b) S. Di Bella, Chem. Soc. Rev. 30 (2001) 355;
(c) S. Barlow, S.R. Marder, Chem. Commun. (2000) 1555;
(d) J. Heck, S. Dabek, T. Meyer-Friedrichsen, H. Wong, Coord. Chem. Rev. 190–192 (1999) 1217;
(e) N.J. Long, Angew. Chem., Int. Ed. Engl. 34 (1995) 21;
(f) D.M. Burland, Chem. Rev. (special issue) 94 (1994) 1–278.
[9] J.A. Mata, E. Peris, J. Chem. Soc., Dalton Trans. (2001) 3634.
[10] (a) W. Figueroa, M. Fuentealba, C. Manzur, D. Carrillo, A.I. Vega, J.-Y. Saillard, J.-R. Hamon, Organometallics 23 (2004) 2515;
(b) C. Manzur, L. Millán, W. Figueroa, D. Boys, J.-R. Hamon, D. Carrillo, Organometallics 22 (2003) 153.
[11] D. Astruc, S. Nlate, J. Ruiz, Modern Arene Chemistry, in: D. Astruc (Ed.), Wiley-VCH, Weinheim, 2002, p. 400 (Chapter 12).
[12] T. Farrell, T. Meyer-Friedrichsen, M. Malessa, D. Haase, W. Saak, I. Asselberghs, K. Wostyn, K. Clays, A. Persoons, J. Heck, A.R. Manning, J. Chem. Soc., Dalton Trans. (2001) 29.
[13] S. Barlow, H.E. Bunting, C. Ringham, J.C. Green, G.U. Bublitz, S.G. Boxer, J.W. Perry, S.R. Marder, J. Am. Chem. Soc. 121 (1999) 3715.
[14] (a) W.H. Morrison, E.Y. Ho, D.N. Hendrickson, Inorg. Chem. 14 (1975) 500;
(b) J.-R. Hamon, D. Astruc, P. Michaud, J. Am. Chem. Soc. 103 (1981) 758.
[15] Y.S. Sohn, D.N. Hendrickson, H.B. Gray, J. Am. Chem. Soc. 93 (1971) 3603.
[16] For a reference gathering a large number of interatomic and metal–ligand distances obtained from the Cambridge Crystallographic Data Base Centre, see A.G. Orpen, L. Brammer, F.H. Allen, D. Kennard, D.G. Watson, R. Taylor, J. Chem. Soc., Dalton Trans. (1989) S1.
[17] (a) J.A. Mata, E. Peris, R. Llusar, S. Uriel, M.P. Cifuentes, M.G. Humphrey, M. Samoc, B. Luther-Davies, Eur. J. Inorg. Chem. (2001) 2113;
(b) A. Togni, M. Hobi, G. Rihs, G. Rist, A. Albinati, P. Zanello, D. Zech, H. Keller, Organometallics 13 (1994) 1224;
(c) I.S. Lee, Y.K. Chung, J. Mun, C.S. Yoon, Organometallics 18 (1999) 5080.
[18] (a) W. Figueroa, M. Fuentealba, C. Manzur, D. Carrillo, J.A. Mata, J.-R. Hamon, J. Chil. Chem. Soc. 48 (2003) 75;
(b) C. Manzur, L. Millán, W. Figueroa, J.-R. Hamon, J.A. Mata, D. Carrillo, Bol. Soc. Chil. Quim. 47 (2002) 431;
(c) C. Manzur, E. Baeza, L. Millán, M. Fuentealba, P. Hamon, J.-R. Hamon, D. Boys, D. Carrillo, J. Organomet. Chem. 608 (2000) 126.
[19] D. Astruc, Chem. Rev. 88 (1988) 1189.
[20] P. Zanello, in: Togni A., Hayashi T. (Eds.), Ferrocenes: Homogenous Catalysis, Organic Synthesis, Materials Science, Wiley-VCH, Weinheim, 1995, p. 317 (Chapter 7).
[21] Reference [5], Chapter 2, Electrochemistry, p. 89.
[22] A.-C. Ribou, J.-P. Launay, M.L. Sachtleben, H. Li, C.W. Spangler, Inorg. Chem. 35 (1996) 3735.
[23] (a) Y. Portilla, I. Chávez, V. Arancibia, B. Loeb, J.M. Manriquez, A. Roig, E. Molins, Inorg. Chem. 41 (2002) 1831;
(b) S.-G. Lee, S.S. Lee, Y.K. Chung, Inorg. Chim. Acta 286 (1999) 215;
(c) F. Coat, M.-A. Guillevic, L. Toupet, F. Paul, C. Lapinte, Organometallics 16 (1997) 5988.
[24] A. Ceccon, S. Santi, L. Orian, A. Bisello, Coord. Chem. Rev. 248 (2004) 683, and references therein.
[25] C. Lambert, W. Gaschler, M. Zabel, R. Matschiner, R. Wortmann, J. Organomet. Chem. 592 (1999) 109.
[26] SAINT (Version 5.0), Bruker Analytical X-ray Systems Inc., Madison, WI, 1998.
[27] G.M. Sheldrick, SADABS, Empirical Absorption Program, University of Götingen, Götingen, Germany.
[28] SHELXTL Reference Manual (Version 5.1). Bruker Analytical X-ray Systems Inc., Madison, WI, 1997.